ISSN 1288-1619

CNRS - Université Pierre et Marie Curie - Université Versailles-Saint-Quentin
CEA - ORSTOM - Ecole Normale Supérieure - Ecole Polytechnique

Institut Pierre Simon Laplace
des Sciences de l'Environnement Global

Notes du Pôle de Modélisation

A model intercomparison of equilibrium climate change in response to CO_2 doubling

H. Le Treut (1) and B. McAvaney (2)

(1) IPSL - Laboratoire de Météorologie Dynamique, Paris, France;
(2) Bureau of Meteorology Research Center, Melbourne, Australia

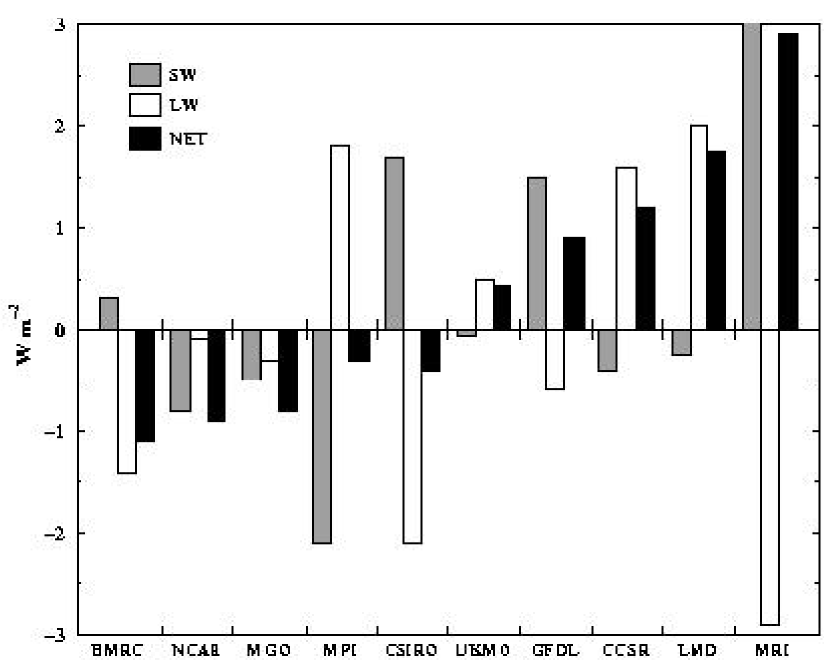

Octobre 2000 **Note n° 18**

CNRS - Université Pierre et Marie Curie - Université Versailles-Saint-Quentin
CEA -CNES - ORSTOM - Ecole Normale Supérieure - Ecole Polytechnique

I P S L

Institut Pierre Simon Laplace
des Sciences de l'Environnement Global

C E T P - LMD - LODYC - LPCM - LSCE - SA

Université Pierre-et-Marie-Curie
B 102 - T15-E5 - 4, Place Jussieu
75252 Paris Cedex 05 (France)
Tél : (33) 01 44 27 39 83
Fax : (33) 01 44 27 37 76

Université Versailles-Saint-Quentin
College Vauban, 47 Boulevard Vauban
78047 Guyancourt Cedex (France)
Tél : (33) 01 39 25 58 17
Fax : (33) 01 39 25 58 22

A simple intercomparison is carried out to investigate the scatter in the simulated equilibrium response of the climate system to a CO2 doubling. The aim of the exercise is to document qualitatively the level of agreement between models. The models are atmospheric models coupled to a simple slab ocean, and the mean response in terms of temperature, precipitation, water vapour and cloudiness is analysed. Some diagnostics regarding the components of the surface and top of the atmosphere (TOA) energetics are also presented. The continuing considerable scatter in results suggests that it would be highly desirable to maintain a central archive repository of model output from all modelling groups so future analyses can be readily performed.

Octobre 2000 , Note n° 18

Directeur de publication : Gérard Mégie, Directeur de l'IPSL
ISSN 1288-1619

A model intercomparison of equilibrium climate change in response to CO2 doubling

H. Le Treut (∗) and B. McAvaney (∗∗)

(*) Laboratoire de Météorologie Dynamique, IPSL, Paris, France.
(**) Bureau of Meteorology Research Center, Melbourne, Australia.

Abstract : A simple intercomparison is carried out to investigate the scatter in the simulated equilibrium response of the climate system to a CO2 doubling. The aim of the exercise is to document qualitatively the level of agreement between models. The models are atmospheric models coupled to a simple slab ocean, and the mean response in terms of temperature, precipitation, water vapour and cloudiness is analysed. Some diagnostics regarding the components of the surface and top of the atmosphere (TOA) energetics are also presented. The continuing considerable scatter in results suggests that it would be highly desirable to maintain a central archive repository of model output from all modelling groups so future analyses can be readily performed.

1. Introduction

The «climate sensitivity» of a model has been formally defined by IPCC to be the global mean temperature change at time of doubling for a model run with a simple slab ocean model. Since the first intercomparison by Cess et al (1989), cloud and water feedbacks are frequently invoked as the most likely explanation for the wide range of climate sensitivity estimates by the various numerical climate models. But little has been done to document -let alone to understand- the comparative behaviour of the different models.

The purpose of the following intercomparison, which was carried out under the recommendation the Working Group of Climate Models (of the World Climate Research Programme), has been to provide a base level description of the scatter in the response of key feedback parameters to a CO2 doubling.
We have chosen to focus on 2CO2 equilibrium experiments, carried out with atmospheric models coupled to an ocean slab of uniform depth, as a good way to explore the differences of behaviour linked with the atmospheric physics only. These experiments therefore do not involve the complexity of the ocean response. They also constitute a reference, and have been carried out (and continue to be) in almost all laboratories, very often with rather recent version of the models.

One might wish to perform a quantitative analysis of the feedback processes acting in the climate scenarios. Adequate methodology has been developed by Wetherald and Manabe (1988) and used with many variants by several modelling groups (e.g. Le Treut et al (1991), Zhang et al (1994) and Colman and McAvaney (1995). Although very powerful, using such techniques has proven to be an impossible task to carry out for the present intercomparison, due to the disparity of model design, particularly in terms of cloud specification for radiative algorithms. Changes in cloudiness, water vapor, surface fluxes and top of the atmosphere (TOA) fluxes constitute a more direct, although very qualitative, method to explore the diversity of the feedbacks between models.

2. Organization of the intercomparison

The intercomparison exercise was mostly carried out during 1998. The participating climate groups were asked to provide key simulated parameters averaged over a few decades (very often 3), for two sets of experiments:

- a control climate (corresponding to «present» conditions, the characterisation of which was left to the authors, as the intention was to use existing simulations)
- a double CO2 climate.

Results were requested for annual means, and winter and summer seasonal averages. The participating groups have been: the Bureau of Meteorology Research Center (BMRC, Australia), the Center for Climate System Research (CCSR, Japan), the Commonwealth Scientific and Industrial Research Organization (CSIRO, Australia), the Geophysical Fluid Dynamics Laboratory (GFDL, USA),), the Goddard Institute for Space Studies (GISS, USA), Hadley Centre (also referenced as UKMO model, UK), the Laboratoire de Météorologie Dynamique (LMD or LMD/IPSL, France), the Max Planck Institute for Meteorology (MPI, Germany), the Meteorological Research Institute (MRI, Japan)), the National Center for Atmospheric Research (NCAR, USA) . The MGO model appears in Figure 8 and is the model of the Main Geophysical Observatory (Russia; see reference in Meleshko et al, 2000)

3. Global and zonal mean changes of the atmosphere

The first striking result of the intercomparison is that it does not show any reduction in the range of model sensitivities to CO2 doubling (Figure 1). The range of 1.5°C to 4.5°C which has been quoted for about 20 years, is still present in our results – with one model even more sensitive. Also, while global precipitation increases in all cases, its relation to global temperature continues to be characterised by a large scatter.

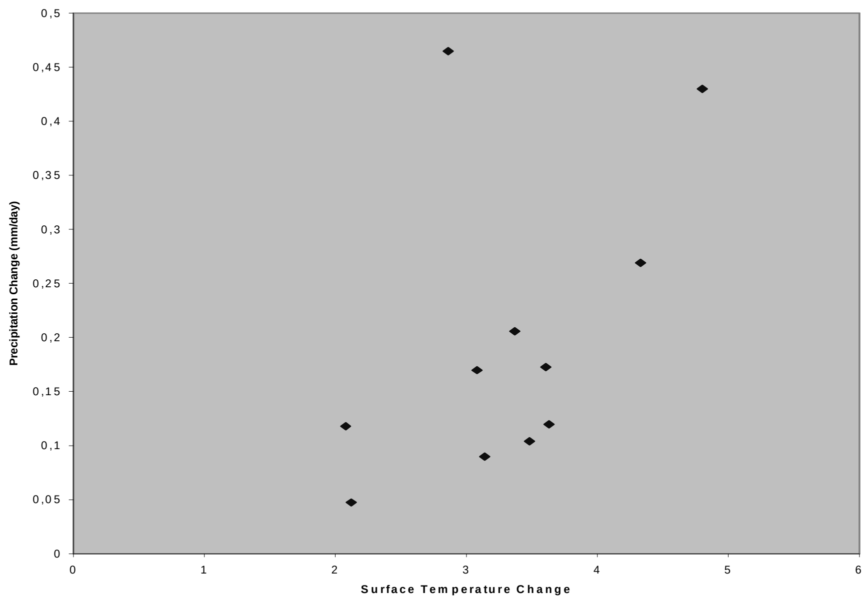

Figure 1: Scatter plot of the global changes in surface temperature and precipitation

In some sense the examination of the of the latitudinal distributions of the mean zonal surface temperature change (Figure 2.a), or the mean zonal precipitation change (Figure 2.b) gives a more balanced impression: there is a clear convergence of the models in terms of pattern, although the amplitude of these patterns differ widely. For surface temperature, the pattern of large temperature changes at high latitudes (presumably associated with snow and ice feedbacks) contrasts with the relatively smaller temperature change in the tropics and sub-tropics. The precipitation changes show systematic increases near the equator and at mid-latitudes, whereas there are often decreases in subtropical areas.

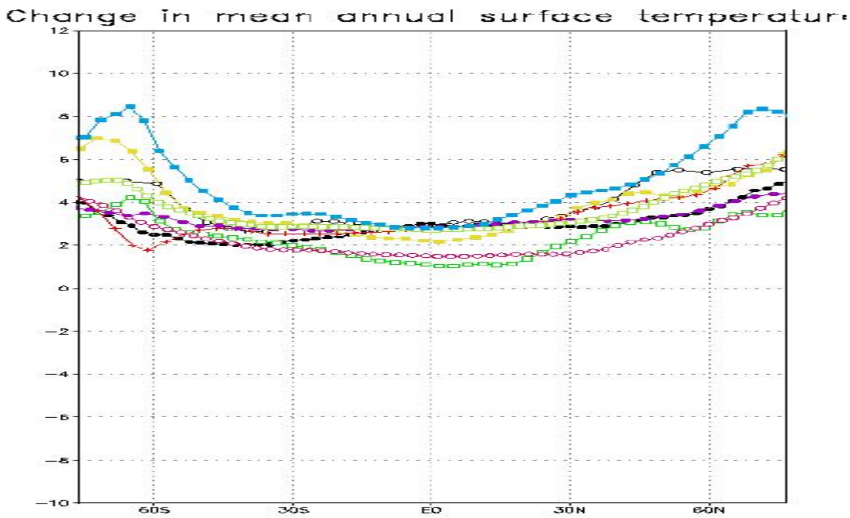

Figure 2.a: Mean zonal surface temperature change for all models

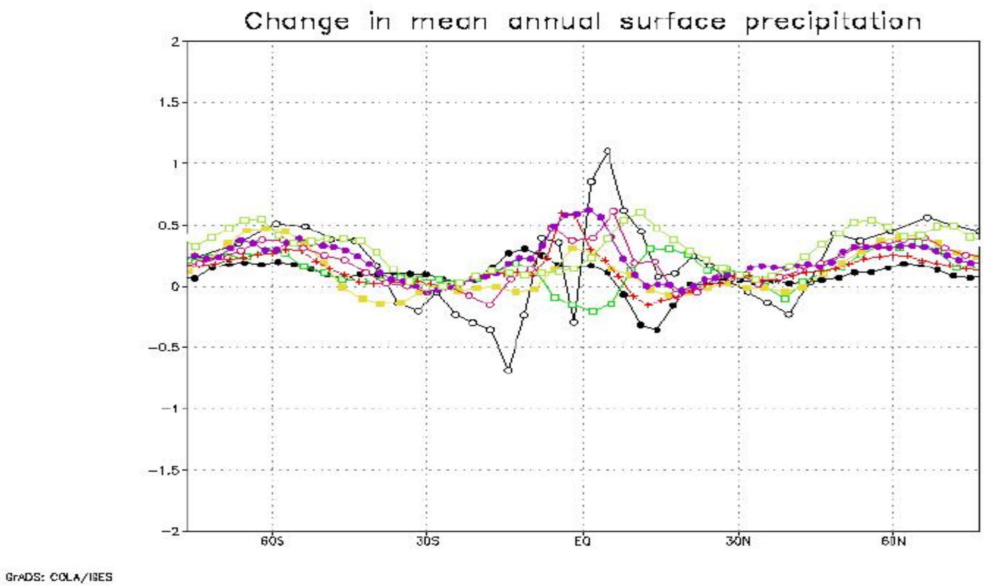

Figure 2.b: Mean zonal precipitation change for all model changes

The mean pattern of the zonal average temperature change through the depth of the atmosphere is displayed for most models in Figure 3. Again the qualitative similarity, and the quantitative scatter is apparent.

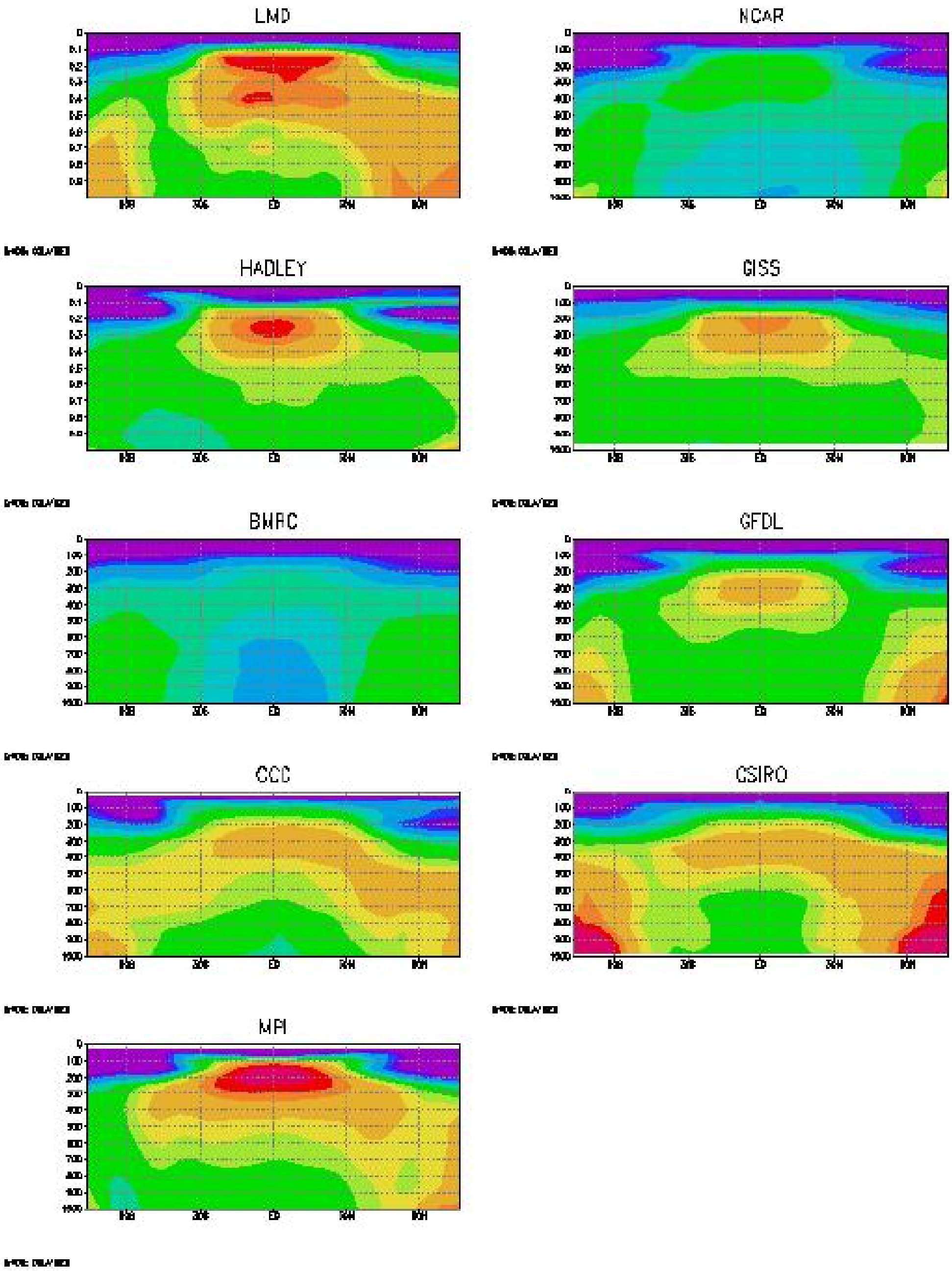

Figure 3: Mean altitude/latitude change of the atmospheric temperature for 9 models. The isolines are every 0.5 K. The colour is the same for all models.

For most models the zonal average temperature change distribution present a pattern with three maxima, one in the upper troposphere at intertropical latitudes and two in the troposphere at high latitudes (at about 60º). These high-latitude warming maxima occur at lower levels: this may reflect the lower level of the tropopause itself, but in some models the maxima extend much closer to the surface. In the previous intercomparison of Schlesinger and Mitchell (1987) where three models were compared, two of them showed a location of the tropical maximum at a much lower altitude, probably in relation with the use of a moist adiabatic adjustment scheme. Such a behaviour does not occur here, but the pattern through which this upper tropospheric tropical warming extends either downward, or poleward, can be quite distinct. A corresponding diversity is present in the pattern and altitude of the stratospheric cooling, in particular at high latitudes.

The magnitude of the maxima can be quite well marked but show considerable variation between models: the upper tropospheric warming varies from about 2 K, to about 8 K, depending on the model. The high latitude warming peaks at levels that range from the surface to 300 hPa, and has a scatter of about 5 K in its amplitude.

Changes in the zonal mean water vapour

Studies by Shine and Sinha (1991) and Hu (1997, 2000) shown that the fractional change in water vapour at a given altitude is a more useful quantity to consider rather than the absolute changes at that altitude. The fractional changes (not shown) of water vapour at higher altitudes is generally larger than at lower altitudes in all models due to the stronger temperature response. Perhaps a more useful indicator of model response is the fractional change of water vapour per degree of warming (Hu, 2000).

The change in the unscaled water vapor pattern (not shown) has rather striking differences in terms of tropical versus extratropical behaviour. In some models the tropical maximum is very marked and probably reflects a marked increase in the lower-layer convergence of water vapour. This marked maximum can extend upwards and is often -although not always- associated with a comparatively smaller moistening of the subtropical areas.

The poleward extension of the moistening is very diverse: the moistening of the high latitude regions (latitudes higher than 50 º or 60 º) is quite insignificant compared to the low latitude, while in a number of models a secondary maximum can occur. This may reflect both the large spread in high latitude temperature response, and also a large variety in the, often crude, treatment of the ice phase in the models.

To illustrate those features in way that allows a more direct model-model comparison we have displayed in Figure 4, vertical profiles of the change in temperature and water vapour averaged over different latitude belts. The colour code for the different models is consistently the same, and shows the strong relation between those two fields. For the tropical domain the moistening extends throughout the depth of the troposphere with a strong gradient from surface to upper troposphere. The high latitude moistening, while small, differs quite remarkably between models with high latitude numerical deficiencies for some models).

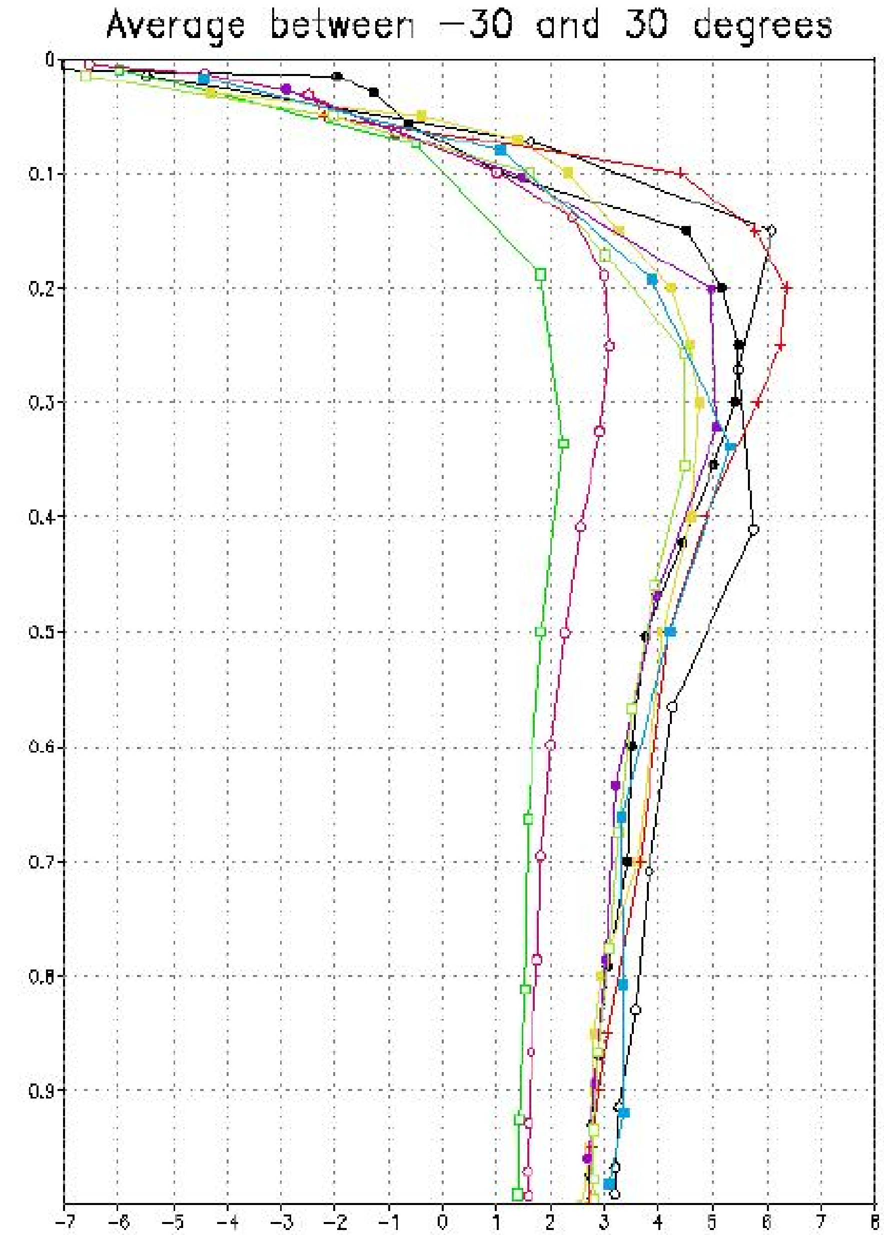

Figure 4.a: Mean vertical profile of the temperature change over the tropical area for all models (in K)

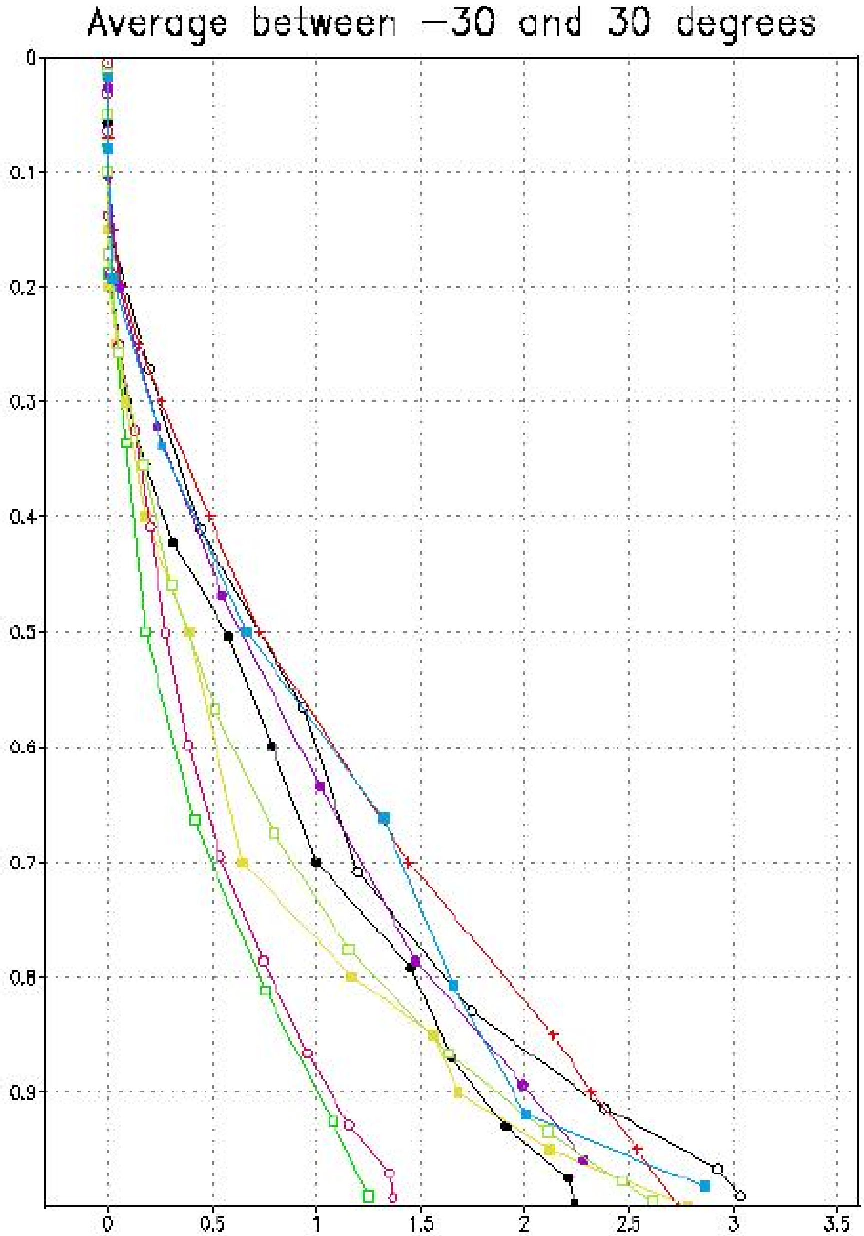

Figure 4.b: Same as Figure 4.a but for water vapour mixing ratio (in g/kg)
(the colour code representing the different models is the same as in 4.a)

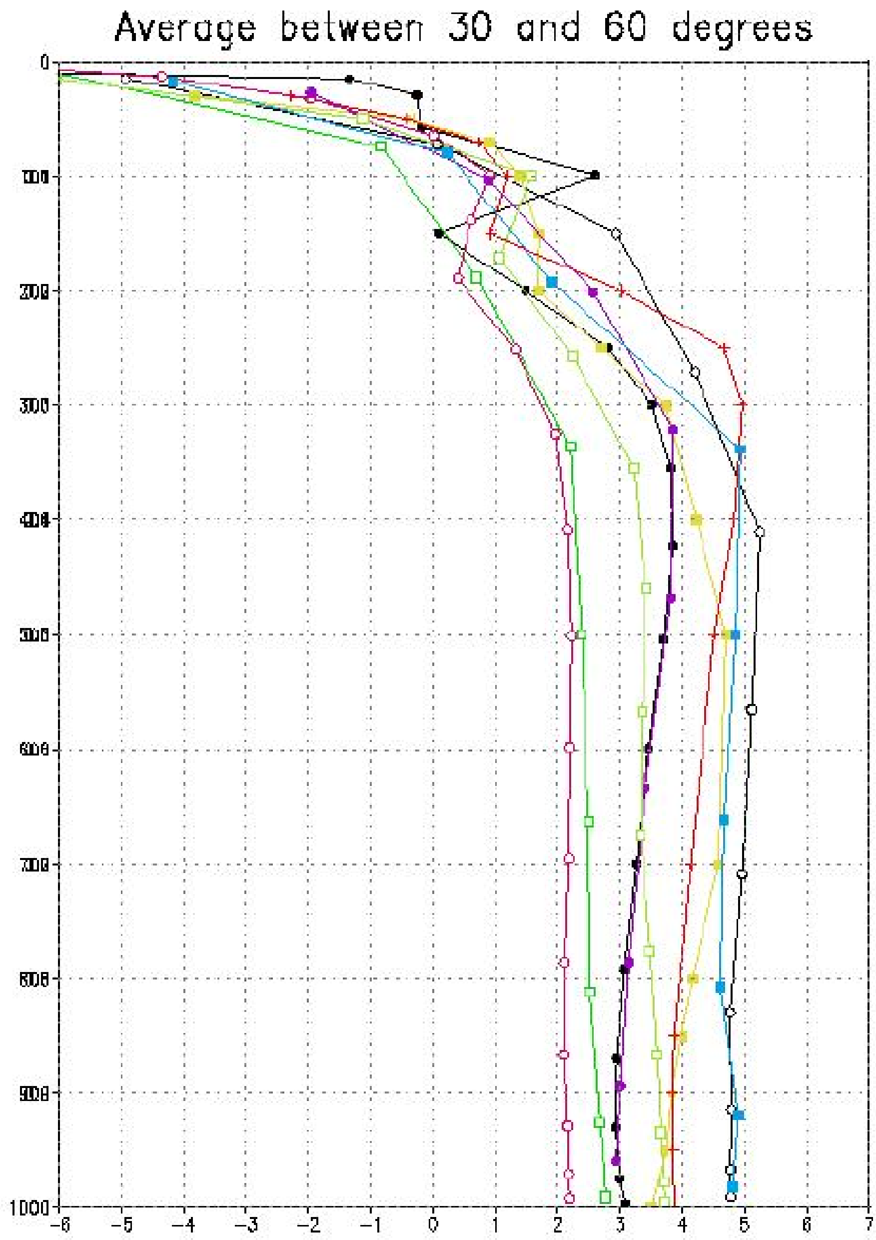

Figure 4.c: Same as Figure 4.a but average for latitudes between 30 º and 60 º.

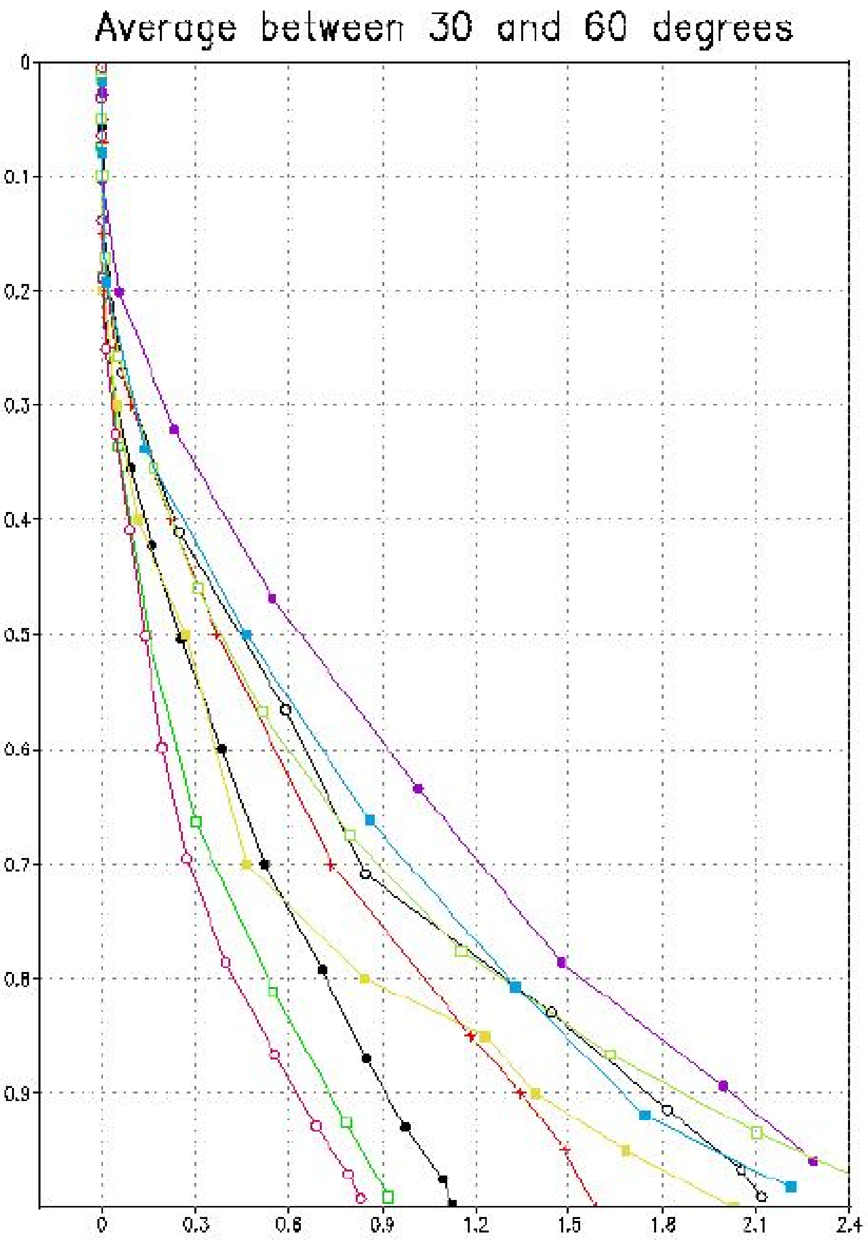

Figure 4.d: Same as Figure 4.b but average for latitudes between 30 and 60 degrees.

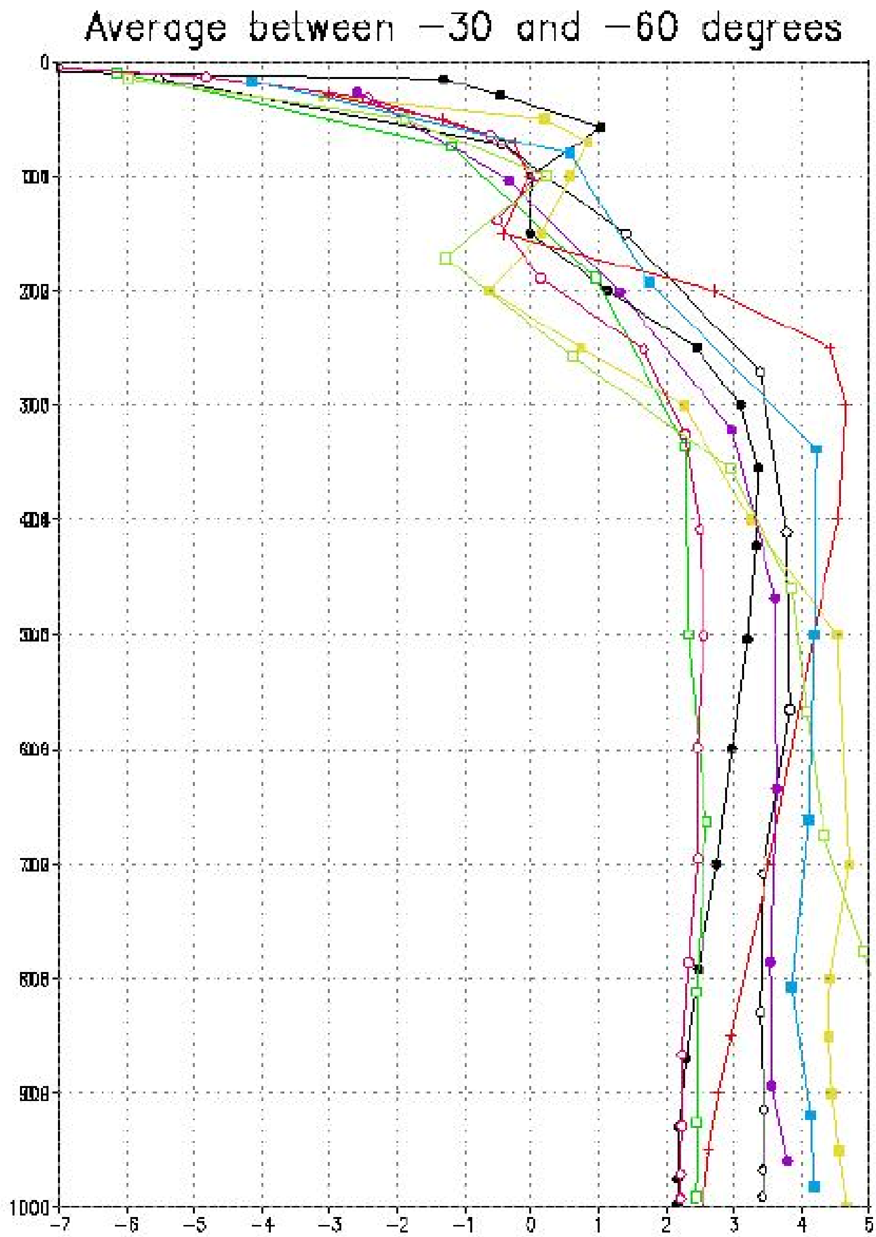

Figure 4.e: Same as Figure 4.a but average for latitudes between -30 and -60 degrees.

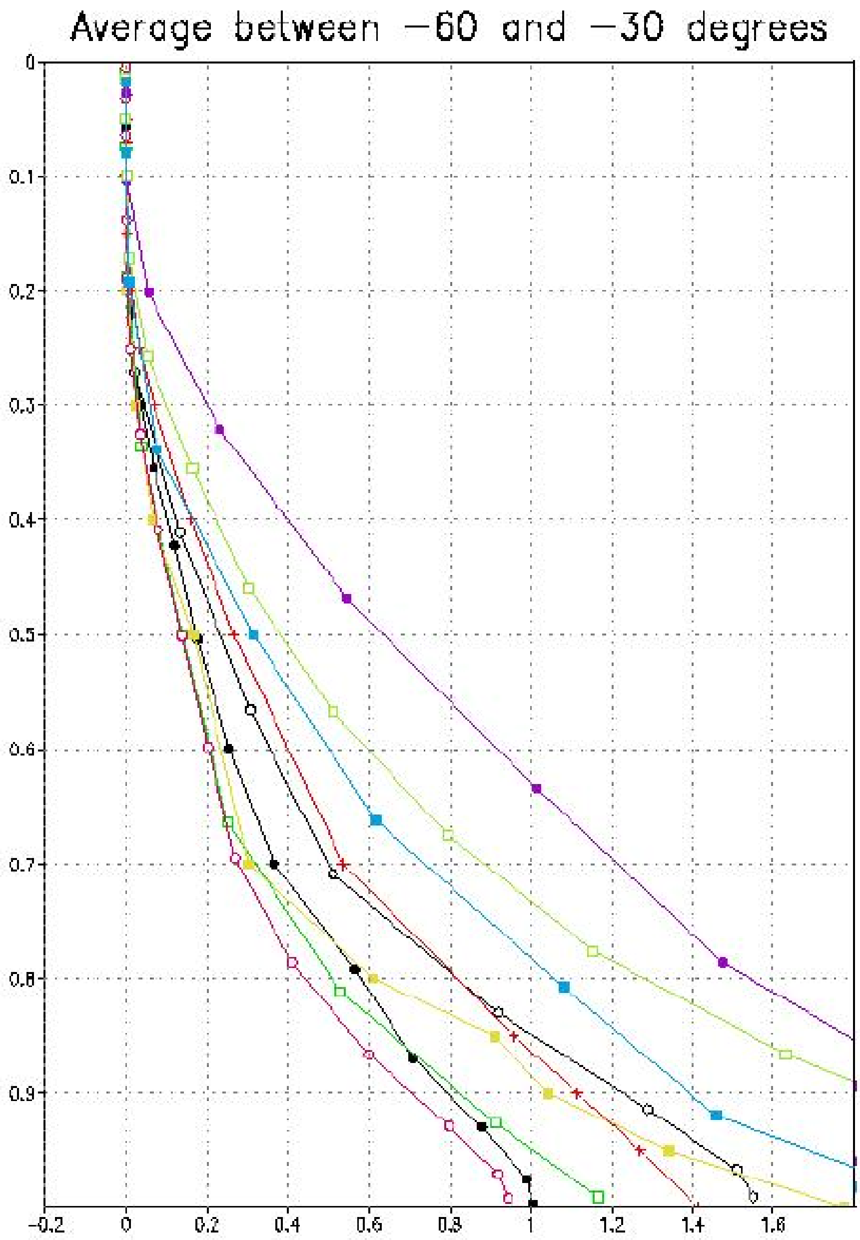

Figure 4.f: Same as Figure 4.b but average for latitudes between -30 and -60 degrees.

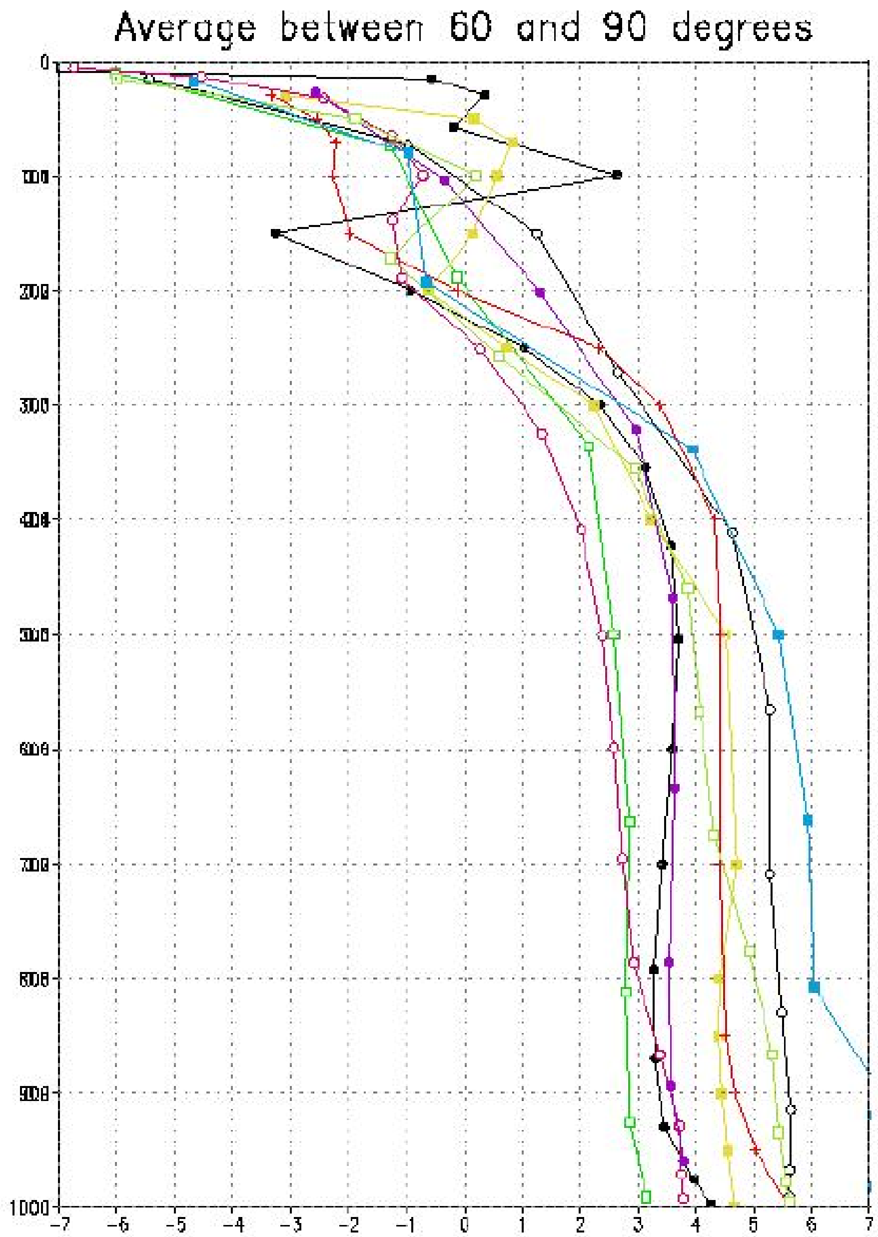

Figure 4.g: Same as Figure 4.a but average for latitudes between 60° and 90 °

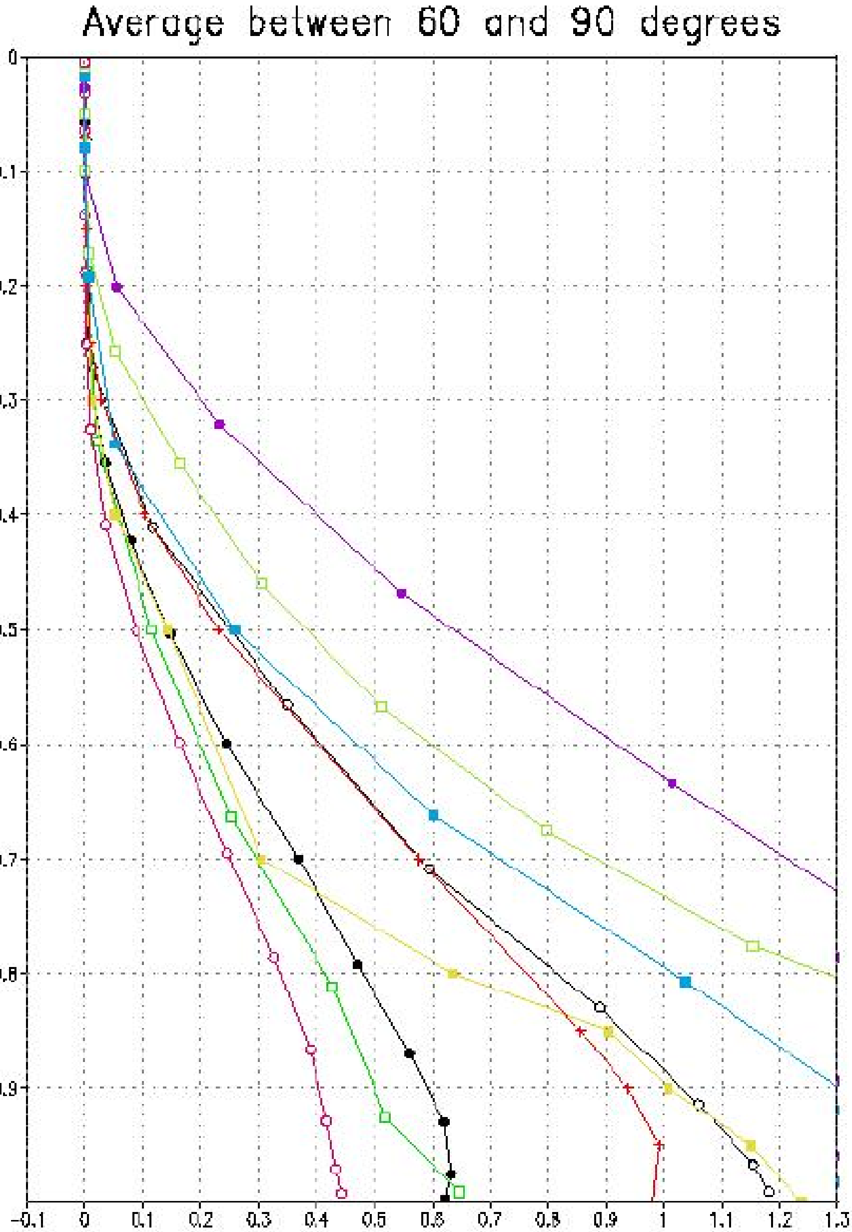

Figure 4.h: Same as Figure 4.b but average for latitudes between 60° and 90°

Cloudiness

In spite of the often stated importance of cloud feedbacks, no direct comparison of cloud response for a range of simulations using different models has been produced to date. In Figure 5 we show the distribution of the mean zonal change in cloud amount for those models where data was available. The models show some broad qualitative similarity, but are sufficiently different in the localisation of the effects to explain the quantitative divergence of the different models. The patterns of cloud changes bear some similarity with the patterns of the relative (or scaled) water vapour change. But cloud increases tend to occur higher up in the atmosphere. Cloudiness also decreases in most models at about 200 or 300 hPa, under the higher troposphere or lower stratospheric temperature change maximum. Some additional features are apparent; in particular in some models (and particularly in the Hadley Centre model, in which this effect was first noted by Senior et al; 1993) there is a cloudiness increase at the ice/liquid transition, which can be explained by the different precipitation properties of the two phases. Also the changes in low Planetary-Boundary Layer Clouds (PBL) are quite distinct from model to model.

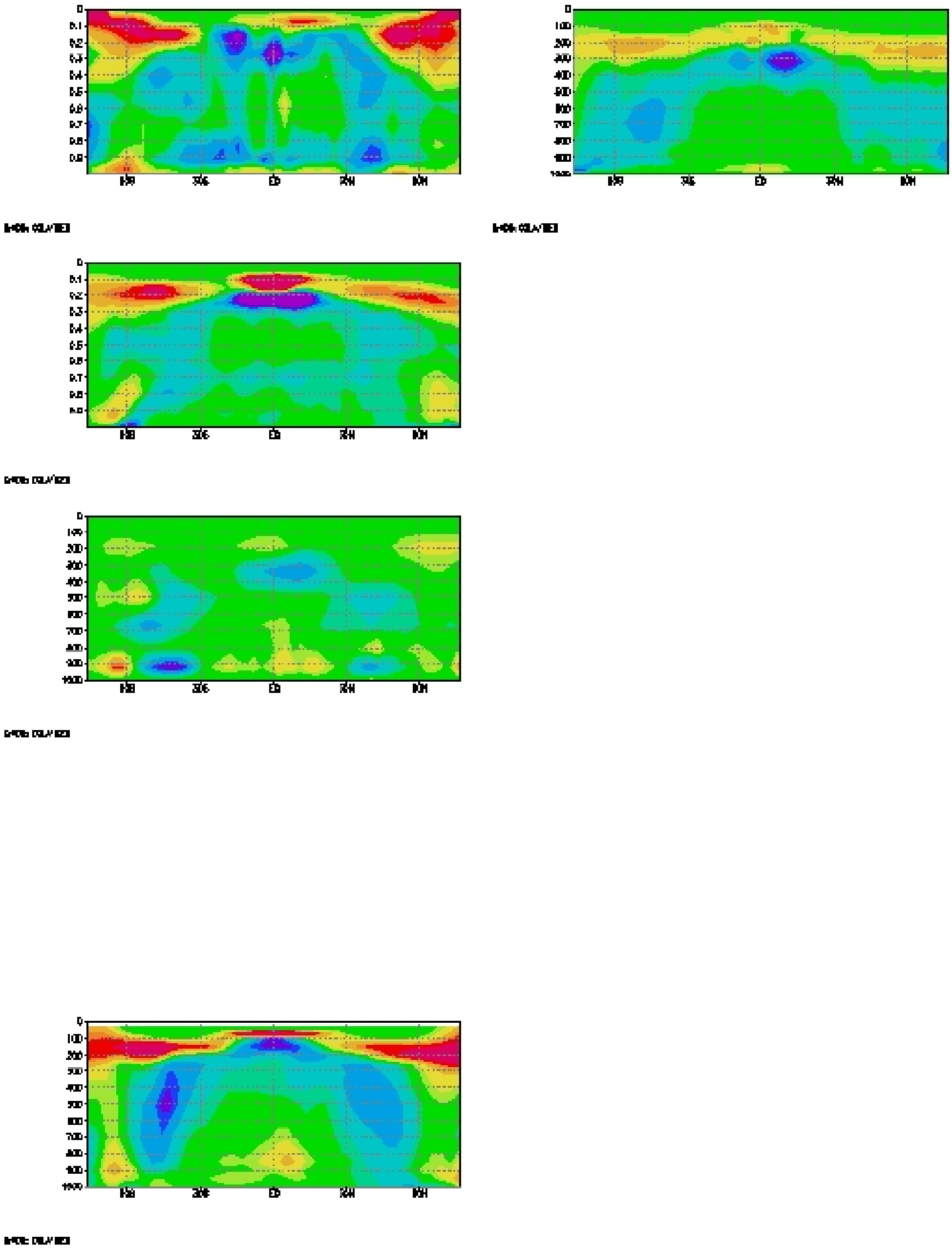

Figure 5: Patterns of mean zonal cloud change distribution for some models (their position in the page matches that of Figure 1)

4.Changes in the fluxes at the TOA and simple diagnostics of the cloud feedbacks

The very large discrepancy between all models in terms of changes in the net radiative fluxes, reflects individual discrepancies in the geographical distribution of the longwave (LW) and shortwave (SW) response (shown in Figure 7 for 5 models, whereas the control values shown in Figure 6 are more similar). Most models react to a temperature increase by some increase in precipitation and cloudiness. But this increase may, or may not, be associated with a displacement of the cloud structures, and can have a very distinct local signature. In addition, it also often corresponds to a different level of compensation between the LW and SW responses (Figure 7). This may vary considerably from model to model depending on the representation of cloud microphysics, and such features as the phase of the condensate, the ice crystal and water droplet equivalent size, or the cloud water content.

The very strong scatter between models is further emphasised by the bar chart found displayed in Figure 8.

Scatter diagrams of the LW and SW responses were plotted for all models (not shown here), as a way to quantify how they may compensate. The comparison with the corresponding changes in cloud radiative forcing (not shown here, because they are not available for all models) confirms that the scatter diagram largely represents the effects of the clouds. While there is some broad agreement in terms of the mean slope, which is positive in all cases, it is difficult to proceed deeper with the limited information available. The scatter diagrams corresponding to the various models show quite distinct patterns, with some plots showing different clusters associated with different geographical regions.

Trying to assess this relation between the LW and SW sensitivity by using observations (mainly satellite measurements), is a key issue. We have tried to use the seasonal cycle as a proxy for climate changes. But we have not found very clear relations between the LW and SW regression at these time scales. In the case of seasonal changes, it is necessary to separate the LW and SW changes which results from a horizontal displacement of the structures from those which really correspond to thermodynamical feedbacks. The limited parameters at our disposal for this task (mainly precipitation) did not prove universal enough from model to model and a more thorough study is necessary , as demonstrated by the results of Bony et al. (1997).

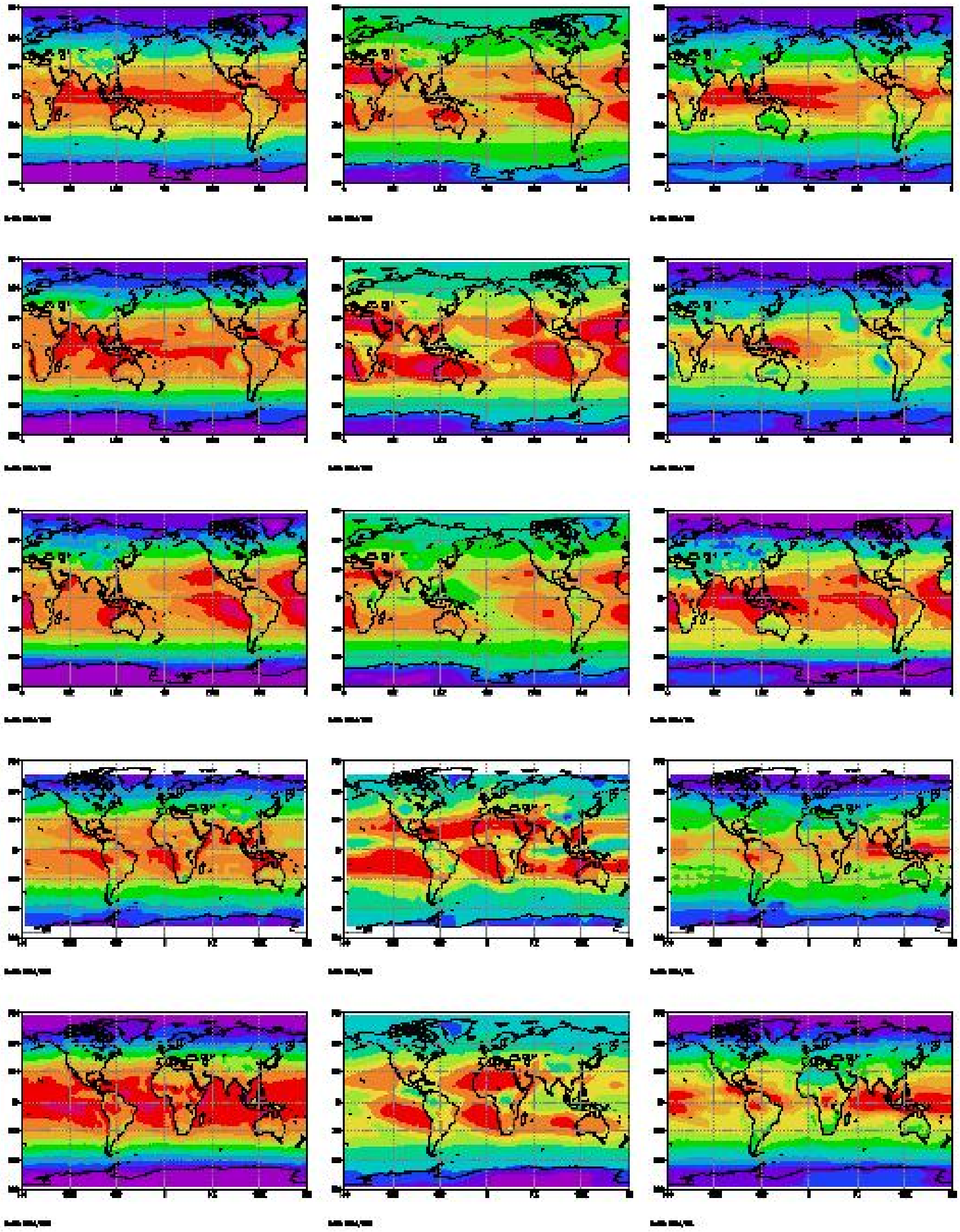

Figure 6: The TOA SW absorbed radiation (left column), the OLR (middle column), and the net radiation at the TOA (right column) for 5 models chosen for their different response to CO2 increase (from top to bottom: HADLEY, BMRC, MPI, NCAR, GISS)

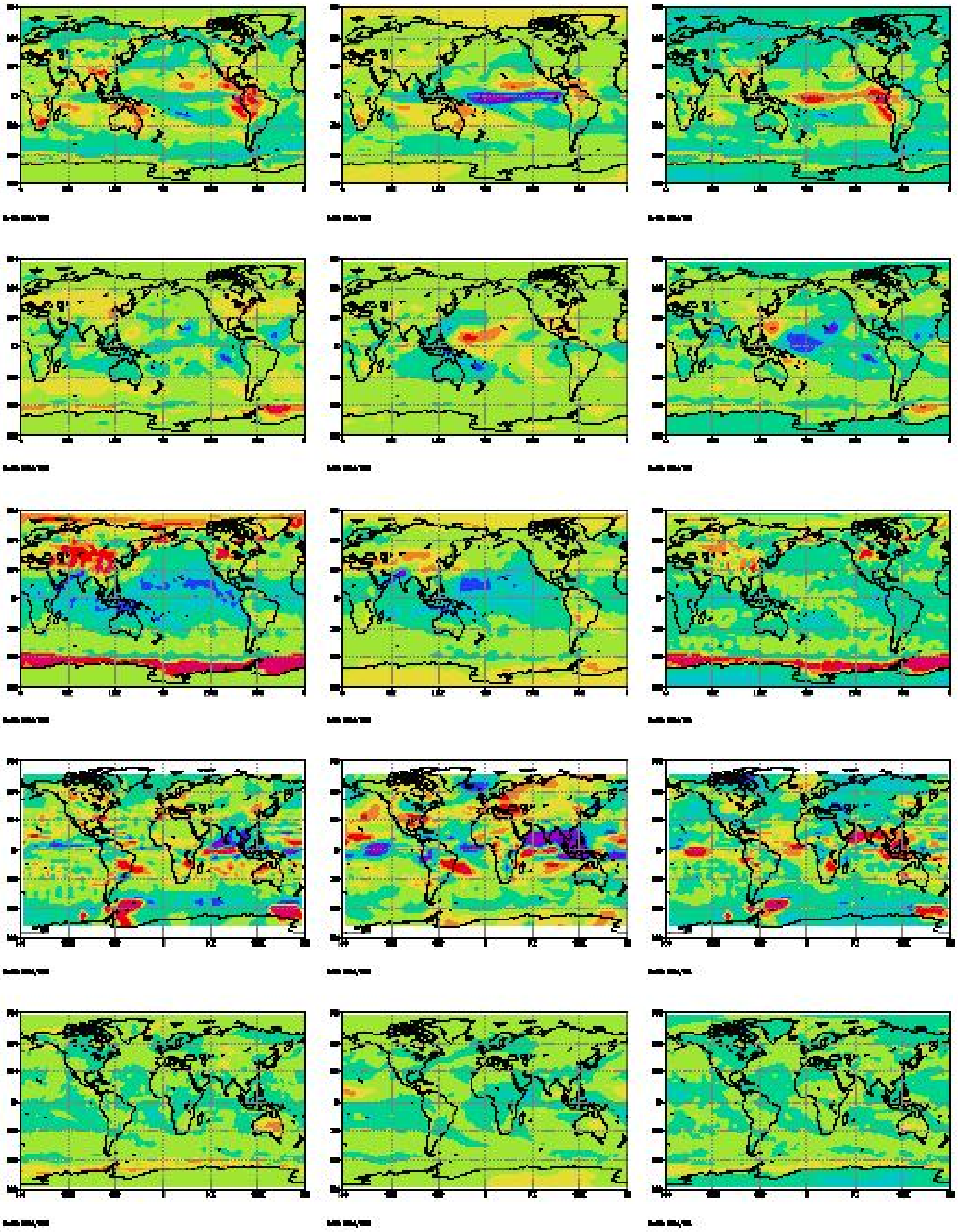

Figure 7: Same quantities as in Figure 6, but change between 2CO2 and 1CO2.

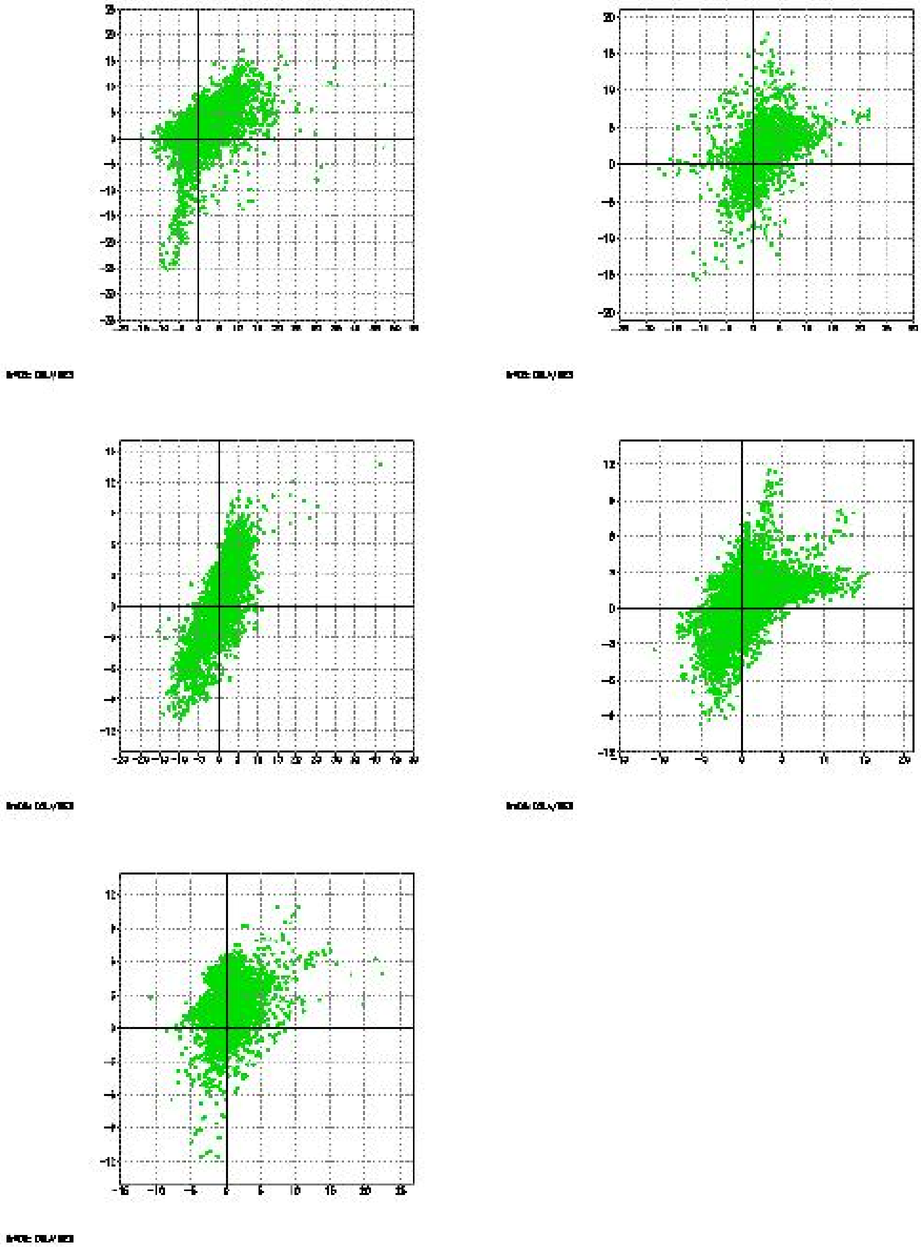

Figure 8: Scatter plot of the changes in respectively the LW and SW radiation at the TOA, for the same models shown in Figure 7.

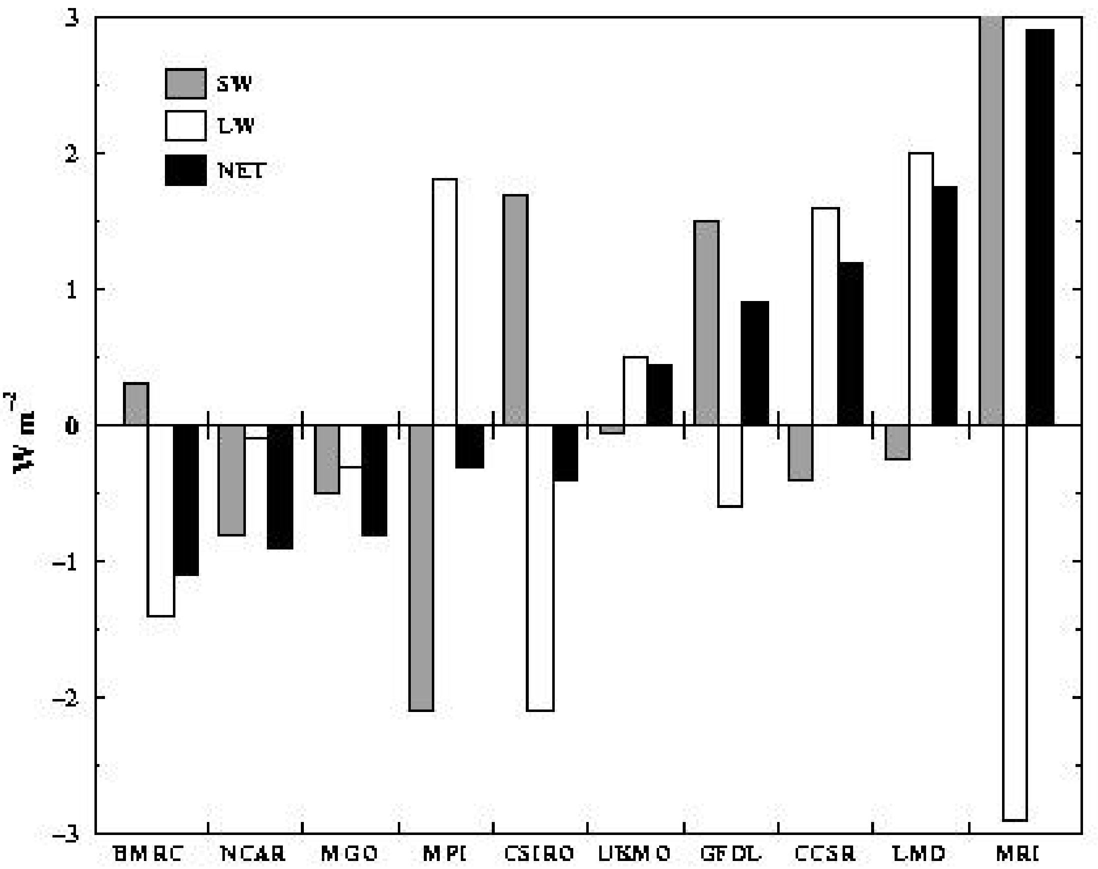

Figure 9: Change in the Top of the Atmosphere (TOA) Cloud Radiative Forcing (CRF). Results presented in the diagram are bounded by a 3 Wm^{-2} limit. This diagram was redrawn for the IPCC report and the model of the MGO (Main Geophysical Observatory, St Petersburg, Russia) was added.

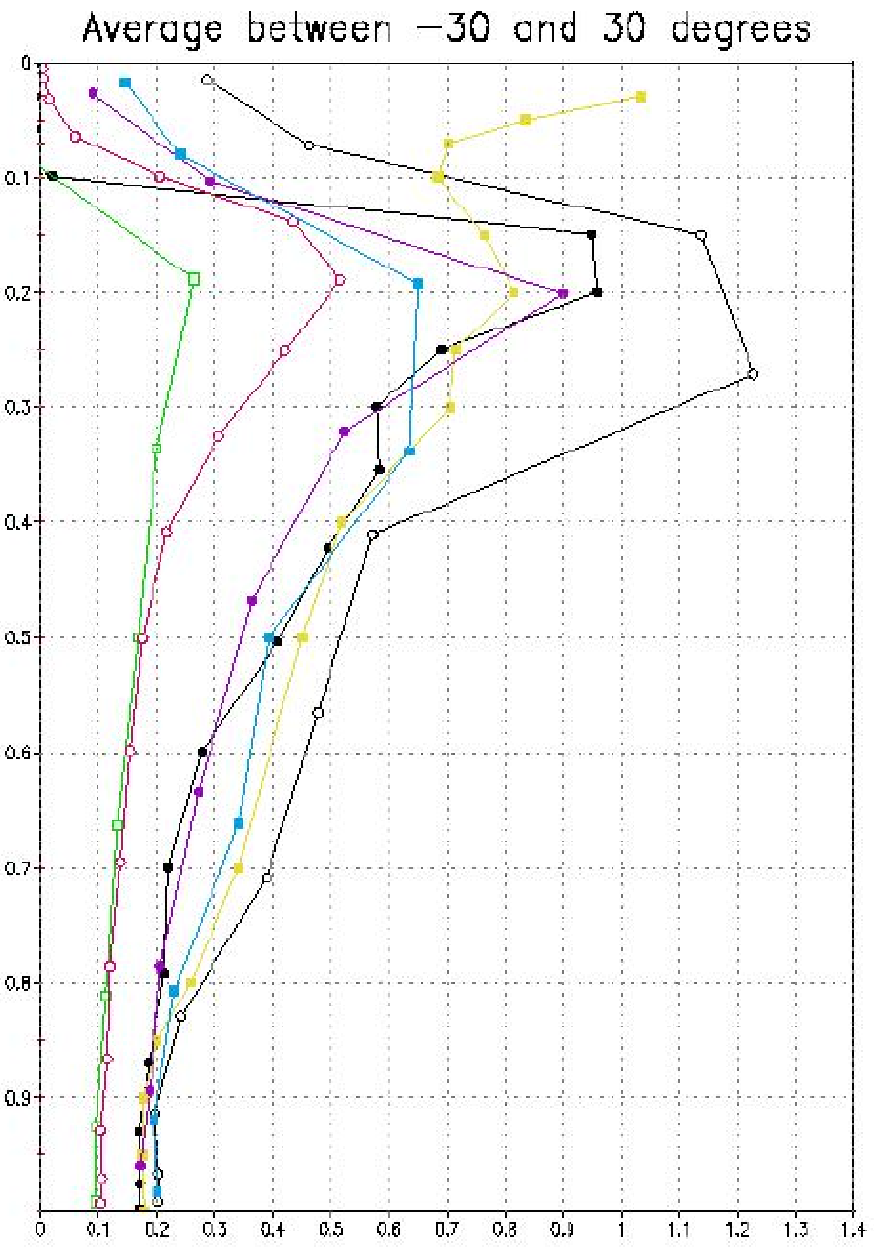

Figure 10 : Same as Figure 4.b, but the water vapour change is scaled by the water vapour mixing ratio of the control simulation (prior to the zonal averaging)

5. Surface Energy Budget

For a long term average and for a model that conserves energy and is in equilibrium the average surface energy budget equation is:
$S + F + \lambda E + H + A = N = 0$
where S is the net solar and F the net long wave radiative flux at the surface, λE is the latent and H the sensible heat flux and A represents the transport of energy in the ocean and in a simple «slab ocean» model (as here) is the specified «Q-flux». N represents a residual term which may include errors and model inconsistencies; it normally is quite small. Over long time scales we can further approximate the energy balance equation so that the net radiation at the surface (R_n) is partitioned into sensible and latent heat fluxes.
$R_n = H + \lambda E + A$

The global and annual averages of the terms in surface energy budget equation have been analysed for all models and show that all models are roughly similar and in line with the observational estimates although there is considerable scatter amongst the models which may exceed the uncertainty in the observations. The models are generally within 25 W/m^2 of the observed for the upward and downward components and within 15 W/m^2 for the net radiation at the surface.

A good approximation to the proportion of the net surface radiation that is channelled into latent heat can be obtained through consideration of the Priestly and Taylor (1972) hypothesis for saturated surfaces as outlined by Garratt (1995) and Garratt *et al* (1993) :
$\lambda E = \beta \Gamma R_n$
where β is about 1.26 and Γ is a function of temperature (varying from 0.56 to 0.99 over the temperature range 283K to 303K). Thus for saturated surfaces it is expected that some 70%-100% of the net surface radiation is used to cool the surface by evaporation. The model results in Table I conform to this general expectation.\

Changes in surface energy budget

The difference between the $2xCO_2$ and $1xCO_2$ surface energy budgets is :
$\delta R_n = \delta H + \lambda \delta E$
where δR_n ($\delta S + \delta F$) is the change in net surface radiation.

Globally and annually averaged values of these difference terms are presented in Table 2. All models behave in the same general qualitative sense in terms of changes in the net surface radiation latent and sensible heat fluxes. There is an extra amount of net surface radiation which is balanced by extra cooling due to latent heat, there is a slight amount of additional warming due to sensible heat. The increased warming due to the change in sensible heat is to be expected since the overall warming of the lower troposphere in the $2xCO_2$ climate tends to increase the stability. There is considerable scatter in the magnitudes of the terms.

The annual mean zonal differences also show considerable variation in detail of the amplitude of terms among the models but overall there is a remarkable qualitative consistency. There are of course differences in the behaviour of these terms over the ocean and over the land but lack of a land sea mask for all models has precluded a detailed inter-model comparison.

Table 1 : TOA or surface energy budget

	Ukmo	Bmrc	Ncar	Giss	Lmd	Gfdl	Ccc	Ccsr	Csiro
OLR	240.4	231.1	236.6	236.0	240.4	233.7	233.6	229.8	239.5
ASR	243.3	230.3	237.0	236.9	252.1	233.6	236.1	232.7	239.5
P	2.9	2.9	3.1	3.5	3.6	2.4	2.7	2.6	2.8
T_a	286.3	287.6	285.8	287.0	288.8	285.3	287.7	287.7	287.1
R_n	116.6	104.7	110.0	124.7	130.4	93.3	91.9	91.9	104.7
λE	92.3	89.9	88.8	100.4	104.0	70.9	75.2	75.2	80.9
H	20.6	20.4	20.8	23.2	19.5	21.7	14.9	14.9	23.0
LW^{up}	394.5	394.9	392.9	385.0	394.8	398.3	383.4	388.9	395.8
LW^{dn}	334.9	342.7	333.4		342.9	330.0	314.5	323.8	337.2
SW	183.9	156.9	171.5		182.2	161.5	156.6	156.6	162.3
LW	59.5	52.3	61.5		51.9	68.3	68.9	64.7	58.6

Table 2 : Change in the energy surface parameters

	Ukmo	Bmrc	Ncar	Giss	Lmd	Gfdl	Ccc	Mpi	Csiro
δP	0.046	0.048	0.118	0.172	0.173	0.206	0.105	0.09	0.269
δT_a	2.86	2.12	2.08	3.09	3.61	3.38	3.48	3.16	4.33
δR_n	4.37	2.19	2.26	3.07	3.15	4.70	1.44		6.92
$\lambda\ \delta E$	5.53	1.88	3.43	4.98	5.02	5.98	3.03		7.83
δH	-0.98	-0.37	-1.31	-1.65	-2.50	-1.22	-1.82		-0.97
δLW^{up}	24.26	11.47	10.45			17.49			22.77
δLW^{dn}	19.56	13.24	13.55			20.82			25.79
δSW	-0.36	0.41	-0.84		-2.25	1.37	-2.35		3.91
δLW	-4.70	-1.78	-3.10		-5.40	-3.33	-3.80		-3.01

6. Conclusion

This study was clearly exploratory, and highlights the great benefits that would ensue from being carried out in a more systematic way especially taking into account the continuous progress of the models in various research centres.

Overall the performance of the different models is marked by two characteristics :

- a general qualitative agreement in the appreciation of the large-scale structure of the atmospheric response to a warming, both in the vertical distribution of these changes and in their latitudinal pattern
- a quantitative disagreement on the amplitude of this response, and its more « local » details

As a result there has probably been no recent reduction in the uncertainty affecting the current estimations of the future warming.

A key factor is the cloudiness response. Although its zonal structure seems broadly consistent between models, its radiative impact is clearly a source of considerable divergence. These divergences are sufficiently large to believe that they could be reduced quite effectively by a programme that would consider in a dedicated manner the issue of model validation through observed satellite data.

References

Boer, G.J., 1993, Climate Change and the regulation of the surface moisture and energy Budgets, Climate Dynamics, 8, 225-239.

Bony S., Duvel J.P., Le Treut H., 1995: Observed dependence of the water vapour and clear-sky greenhouse effect on sea surface temperature : comparison with climate warming experiments, Climate Dynamics, 11, 307-320.

Bony S., K.-M. Lau and Y.C. Sud, 1997: Sea-Surface Temperature and Large-Scale Circulation Influences on Tropical Greenhouse Effect and Cloud Radiative Forcing, J. Climate, 10, 2055- 2077.

Cess, R.D, G.L. Potter and Coauthors, 1989: Interpretation of Cloud-Climate Feedback as Produced by 14 Atmospheric General Circulation Models, Science, 245, 513-516.

Cess, R. D. and 29 co-authors, 1993: Uncertainties in carbon dioxide radiative forcing in atmospheric general circulation models. Science, 262, 1252--1255.

Gutowski, W.J., Gutzler, D.S., Wang. W.-C., 1991, Surface Energy Budgets of three General Circulation Models: Implications for simulating regional climate change. J Climate, 4, 121-134.

Hu H., 1996, Water vapour and temperature lapse rate feedbacks in the mid-latitude seasonal cycle, Geophys. Res. Lett., **23**,1761-1764.

Hu, H, R.J. Oglesby and B Saltzman, 2000, The relationship between atmospheric water vapor and temperature in simulations of climate change, Geophys. Res. Lett. 27, 3513-3516

Schlesinger M.E. and J.F.B. Mitchell, 1987: Climate model simulations of the equilibrium climatic response to increased carbon dioxide, Rev. Geophys., 25, 760-798.

Shine, K.P. and A. Sinha, 1991, Sensitivity of the Earth’s climate to height dependent changes in the water vapour mixing ration, Nature, **354**, 382-384.

Watterson, I.G. and M.R. Dix, 1996, Influences on surface energy fluxes in simulated present and doubled CO_2 climates. Climate Dynamics, 12, 359-370.

Déjà paru :

5 : Avril 1998 O. Aumont, J. C. Orr, P. Monfray, and G. Madec, *Nutrient trapping in the equatorial Pacific: The ocean circulation solution*

6 : Mai 1998 Emmanuelle Cohen-Solal and Hervé Le Treut, *Long term climate drift of a coupled surface ocean-atmosphere model : role of ocean heat transport and cloud radiative feedbacks*

7 : Juin 1998 Marina Lévy, Laurent Mémery and Gurvan Madec, *Combined Effects of Mesoscale Processes and Atmospheric High-Frequency Variability on the Spring Bloom in the MEDOC Area*

8 : Septembre 1998 Carine Laurent, Hervé Le Treut, Zhao-Xin Li, Laurent Fairhead and Jean-Louis Dufresne, *The influence of resolution in simulating inter-annual and inter-decadal variability in a coupled ocean-atmosphere GCM, with emphasis over the North Atlantic.*

9 : Octobre 1998 Francis Codron, Augustin Vintzileos and Robert Sadourny, *An Improved Interpolation Scheme between an Atmospheric Model and Underlying Surface Grids near Orography and Ocean Boundaries.*

10 : Novembre 1998 Z.X. Li and A.F. Carril, *Transient properties of atmospheric circulation in two reanalysis datasets.*

11 : Décembre 1998 Gurvan Madec, Pascale Delecluse, Maurice Imbard and Claire Lévy, *OPA8.1 ocean general circulation model reference manual.*

12 : Janvier 1999 Marc Guyon, Gurvan Madec, François-Xavier Roux, Christophe Herbaut, Maurice Imbard, and Philippe Fraunie*Domain Decomposition Method as a Nutshell for Massively Parallel Ocean Modelling with the OPA Model .*

13 : Février 1999 Eric Guilyardi, Gurvan Madec, and Laurent Terray *he Role of Lateral Ocean Physics in the Upper Ocean Thermal Balance of a Coupled Ocean-Atmosphere GCM*

14 : Mars 1999 D. Hauglustaine *Impact of Biomass Burning and Lightning Emissions on the Distribution of Tropospheric Ozone and its Precursors in the Tropics*

15 : Décembre 1999 L. Menut, R. Vautard, C. Honnoré, and M. Beekmann *Sensitivity of Photochemical Pollution using the Adjoint of a Simplified Chemistry-Transport Model*

16 : Janvier 2000 J.-Ph. Boulanger *The Trident Pacific model. Part 1: The oceanic dynamical model and observations during the TOPEX/POSEIDON period*

17 : Janvier 2000 J.-Ph. Boulanger and Christophe Menkes *The Trident Pacific model Part 2: The thermodynamical model and the role of long equatorial wave reflection during the TOPEX/POSEIDON period*

18 : Octobre 2000 H. Le Treut and B. McAvaney *A model intercomparison of equilibrium climate change in response to CO_2 doubling*

Plus de détails sont disponibles sur Internet :
http://www.ipsl.jussieu.fr/modelisation/liste-notes.html.